Temperature-Dependent Analysis and RF-Model of 10Gbps VCSELs

S. Nuttinck, E. Gebara[*], M. Maeng and J. Laskar

Georgia Institute of Technology, School of Electrical and Computer Engineering, Atlanta, GA 30332,

sn46@prism.gatech.edu

[*] Quellan Inc., 250 14th street, Atlanta, GA

10Gbps Vertical Cavity Surface Emitting Lasers (VCSELs) are fully characterized and modeled at various temperatures of operation from DC to 15GHz. Studying devices under these conditions of operation enables one to acquire a better understanding of the device physics, and permits to build temperature-dependent VCSEL RF models necessary for accurate opto-electronic integrated circuit (OEIC) designs. The extracted model accurately predicts the reflection coefficient up to 15GHz above and below threshold at various biases and temperatures. This is the first time that a temperature-dependent RF model for VCSEL is presented.

I. INTRODUCTION

The rapid development of multimedia communications in recent years calls for ever-increasing bandwidth, data throughput and high capacity transmission [1-2]. These needs could be addressed by improved device technologies, improved modulation techniques, or by expanding the bandwidth of the fiber.

Vertical Cavity Surface Emitting Lasers (VCSELs) offer an easy extension to 2-D arrays, and present very large intrinsic bandwidth due to reduced cavity volume allowing them to be modulated at speeds ranging from DC to several GHz. Additionally, VCSELs offer threshold currents in the few mA range and power efficiencies around 50%. VCSEL technology is promising to address digital communication needs for high-speed short-haul transmissions [3-5].

Models that can accurately predict VCSEL behavior are important in Opto-Electronic Integrated Circuit (OEIC) design because they can be implemented in standard simulation tools allowing optimization for best system performance [6-7].

Integration of the temperature of operation in VCSEL RF-model is of significant interest due to the large temperature coefficients associated to some elements of the VCSEL's equivalent circuit like the threshold current and the series resistance due to the Bragg reflectors.

In Section II, we present the calibration procedures and details of the characterization system used to measure on-wafer RF performance up to 15GHz of VCSELs at cryogenic temperatures. Section III and Section IV analyze respectively the DC and the small-signal modulation characteristics of the VCSEL at various temperatures of operation. Finally, an RF model of a 10Gbps GaAs VCSEL that accurately predicts its characteristics from DC to 15GHz, at different temperature and bias conditions is presented in Section V.

II. EXPERIMENTAL SETUP

RF characteristics of 10Gbs GaAs VCSELs operating at 850nm have been measured from temperatures as low as 150K, up to ambient temperature, using a custom made cryogenic probe station, and a vector network analyzer (8510C) along with a high-speed photo-detector.
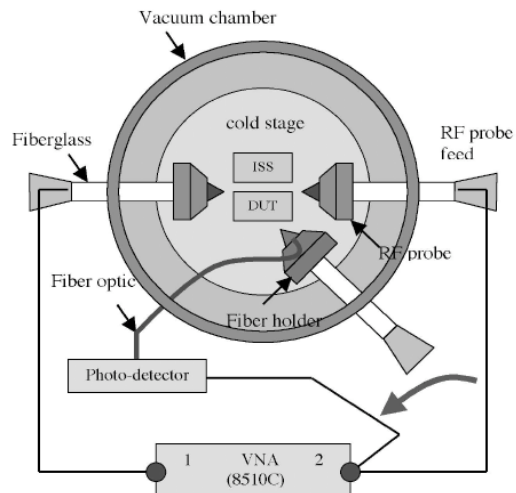

FIG.1: Schematic of the cryogenic microwave probe station for RF characterization of VCSEL.

The cryogenic probing system has initially been developed to investigate and to model high-speed transistors [8]. Successes in extracting accurate temperature-dependent RF models and their employment to MMIC designs impel to apply similar techniques to achieve accurate VCSEL RF models. In order to reach that goal, the cryogenic

system has been modified to meet the needs for RF/Optical measurements. This is achieved by adding a positionner that holds a custom-made fiber optics guide. The device under test (DUT) is mounted on the cold wafer stage and the test chamber is evacuated to prevent frost build up and large thermal gradients when cooling the chamber. To accurately measure the RF performance of the VCSEL up to 15GHz a full two-port calibration is implemented at each temperature of interest. Calibrations are necessary to take into account losses, match errors, and leakage errors of the network analyzer along with all cables, connectors and probes that connect to the DUT. Once the calibration done, Port-2 cable is connected to a 25 GHz photo-detector that samples the optical information from a 62.5μm core multi-mode fiber positioned on top of the VCSEL through the custom-made fiber holder. Fig.1 illustrates the setup used. Photography of a measured VCSEL is shown in Fig.2.
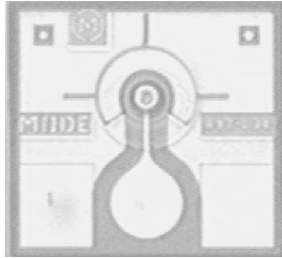

FIG.2: Top-view photography of an 850nm VCSEL.

III. DC MEASUREMENTS AND ANALYSIS RESULTS

The temperature dependent current-voltage characteristics of the 10Gbps VCSEL are shown in Fig. 3. When decreasing the temperature of operation, the junction voltage at a fixed current increases.
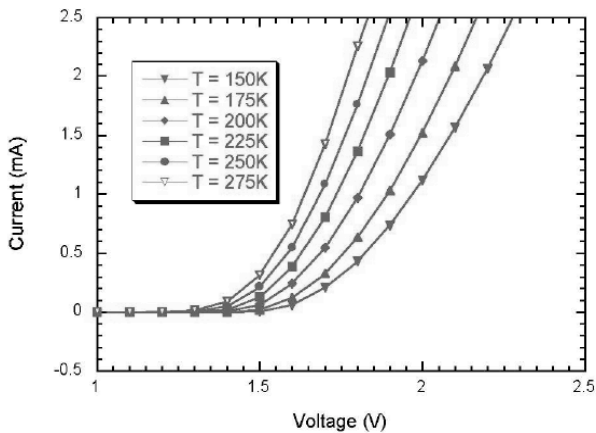

FIG.3: VCSEL IV characteristics measured from T = 150K to T = 275K.

Also, the lasing threshold current in a VCSEL varies with the temperature. It is determined by the

difference between the gain and loss of the active region at the lasing wavelength. Since, the gain of the quantum wells and the resonance of the Fabry-Perot cavity vary at different rates with temperature, the VCSEL threshold current is minimum at a temperature where the peak of the quantum well emission coincides with the cavity resonance. When the temperature is either raised or lowered from this optimum condition the VCSEL current threshold increases. In our case, the VCSEL is optimized for room temperature operation..

IV. SMALL-SIGNAL MODULATION MEASUREMENTS AND ANALYSIS RESULTS

Fig. 4 and Fig. 5 illustrate the forward transmission and reflection coefficient for different bias conditions at T = 300K, and at T = 150K.
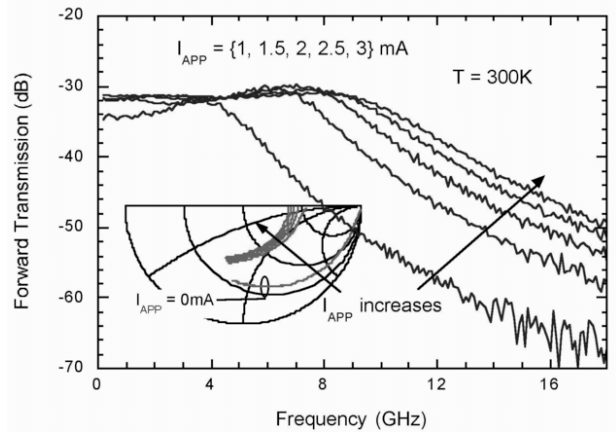

FIG.4: Measured VCSEL forward transmission and reflection coefficient under different bias conditions at T = 300K.
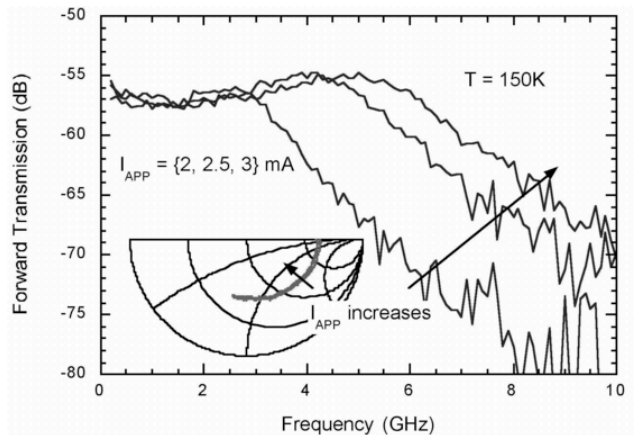

FIG.5: Measured VCSEL forward transmission and reflection coefficient under different bias conditions at T = 150K.

The total inversion rate equation of a semiconductor laser is used to determine the optical response of a VCSEL to a small-signal modulation. It can be expressed [9]:

$$\frac{\Delta\phi}{\Delta J} = \frac{\phi_0 + \beta/\tau_S}{\left[(\sigma_S \cdot \phi_0 + \beta/\tau_S)/\tau_P - \omega^2\right] + j\omega\left[1/\tau_S + \sigma_S \cdot \phi_0\right]}$$

where ϕ_0 represents optical power due to the applied current J_0, and $\Delta\phi$ corresponds to the variation of the number of photons due to a small-signal modulation ΔJ of the current. β is the fraction of spontaneous emission to couple into the mode TEM_{00}, τ_S is the spontaneous recombination lifetime of the carriers, τ_P is the photon lifetime, and σ_S is a collection of constants. The critical frequency (ω_C) that maximizes this ratio can be expressed by:

$$\omega_C^2 = \frac{1}{\tau_P} \cdot \left(\sigma_S \cdot \phi_0 + \frac{\beta}{\tau_S}\right) \approx \frac{\sigma_S \cdot \phi_0}{\tau_P} \qquad (2)$$

This expression confirms that at fixed temperature the maximum modulation frequency increases when operating at higher optical power (Fig.4 and Fig.5). Fig. 6 and Fig. 7 illustrate the forward transmission, and the reflection coefficient at various temperatures of operation under the same bias condition.
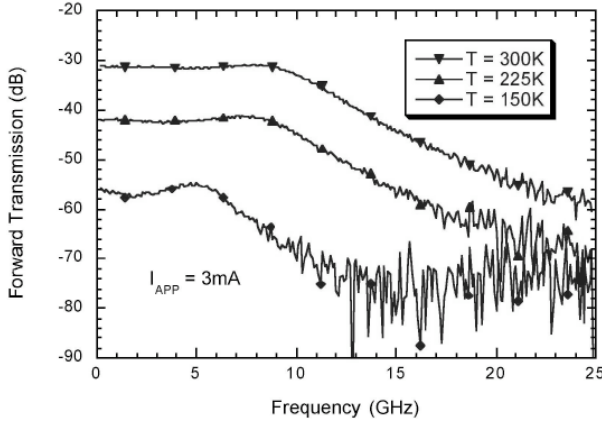

FIG.6: Measured VCSEL forward transmission at T = 150K, T = 225K and T = 300K.

Fig.6 shows that at fixed current the 3dB bandwidth and the forward transmission magnitude degrade when reducing the temperature of operation. The decrease in temperature results in an increase of the lasing threshold current, and therefore in a decrease of the optical power for fixed current, affecting the 3dB bandwidth as described in Eqn.2. The reduction of the forward transmission coefficient magnitude is associated to the measurement setup condition, indeed, as seen in Fig.7, lowering the temperature of operation while keeping the same current condition moves the reflection coefficient further away from the 50-Ohm measurement setup conditions leading to a reduction of the RF optical power forward response.
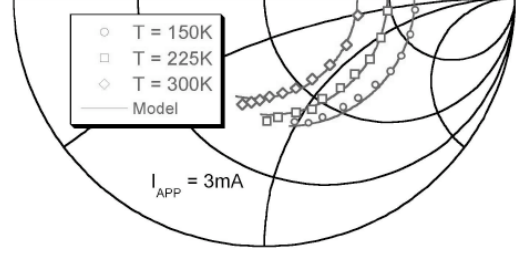

FIG.7: Measured and modeled VCSEL reflection coefficient at T = 150K, T = 225K and T = 300K from DC to 15GHz

V. RF MODELING RESULTS

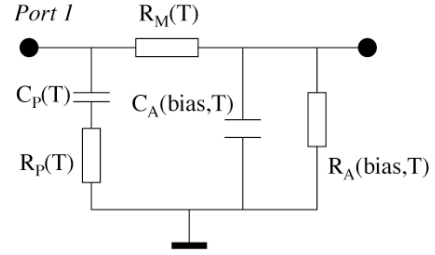A simple equivalent circuit (Fig.8) is used to model the RF characteristics of the VCSEL [10].

FIG.8: Equivalent circuit model for VCSEL.

C_P is the pad capacitance, R_P the pad loss, R_M the mirror resistance, C_A the capacitance of the active region, and R_A the resistance associated to the optical cavity.

The model accurately predicts the RF performance up to 15GHz at different temperatures and biases. Fig.7 shows the measured and simulated reflection coefficient at various temperatures of operation for I_{APP} = 3mA.

The elements that significantly vary with the temperature are R_M, R_A, and C_P. Their extracted values for I_{APP} = 3mA are shown in Table 1.

Temp. (K)	R_M (Ω)	R_A (Ω)	C_P (fF)
150	180	34	275
275	130	25	240
300	97	16	221

TAB.1: Extracted circuit parameters that significantly vary with the temperature of operation. (I_{APP} = 3mA).

R_M represents the resistance of the Fabry-Perot cavity mirrors. These mirrors are distributed Bragg reflectors, and are composed by a stack of high and low bandgap semiconductor This series of hetero-junctions leads to the existence of a barrier potential and therefore to a temperature dependent voltage drop. As shown in table 1, the VCSEL series resistance (R_M) is high, and its relative variation (85% from 150K to 300K) dominates the temperature dependence of the VCSEL current-voltage characteristics.

Also, temperature-dependent modeling of R_A and C_P cannot be ignored. Their relative variation over the measured temperatures is 112% and 25%, respectively. Herein, the importance of including the temperature coefficients in VCSEL RF models.

VI. CONCLUSION

In this paper we presented techniques for on-wafer temperature-dependent VCSEL RF characterization, along with an analysis of the measurement results. A VCSEL model that accurately predicts the RF characteristics from DC to 15GHz, at different temperature and bias conditions is implemented. This leads to accurate VCSEL RF model necessary for high performance OEIC designs.

REFERENCES

[1] V. Hietala, C. Chun, J. Laskar, K. Choquette, K. Geib, A. Allerman, and J. Hindi, "Two-dimensional 8x8 Photoreceiver Array and VCSEL Drivers for High-Throughput Optical Data Links", GaAs IC Symposium, Seattle, pp.189-192, 2000.

[2] M. Ghisoni, M. Dubois, C. Erikson, J. Isaksson, J. Jonsson, "Parallel Data Communication Links with Throughputs up to 30Gbit/s", Swedish National Symposium on GigaHertz Electronicts, Goteborg, Sweden, pp. 241-244, 2000.

[3] J. Tatum, A. Clark, J. Guenter, R. Hawhorne, and R. Johnson, "Commercialization of Honeywell's VCSEL Technology", Proceedings of the SPIE Vol. 3946, pp. 2000.

[4] U. Fiedler, G. Reiner, P. Schnitzer, and K. Ebeling, "Top Surface-Emitting Vertical-Cavity Laser Diodes for 10-Gb/s Data Transmission", IEEE Photonic Technology Letters, Vol. 8, No. 6, pp. 746-748, June 1996.

[5] R. Michalzik, P. Schnitzer, U. Fiedler, D. Wiedenmann, and K. Ebeling, "High-Bit Rate Data Transmission with Short-Wavelength Oxidized VCSEL's: Toward Bias-Free Operation", Journal of Selected Topics in Quantum Electronics, Vol. 3, No. 2, pp. 396-404, April 1997.

[6] M. Bruensteiner, G. Papen "Extraction of VCSEL Rate-Equation Parameters for Low-Bias System

Simulation", IEEE Journal of Selected Topics in Quantum Electronics, Vol. 5, No. 3, pp. 487-494, May/June 1999.

[7] P. Mena, J. Morikuni, S. Kang, A. Harton, and K.Wyatt, "A Simple Rate-Equation-Based Thermal VCSEL Model", Journal of Lightwave Technology, Vol. 17, No. 5, pp. 865-872, May 1999.

[8] J. Laskar, J.J. Bautista, M. Nishimoto, M. Hamai, R. Lai, "Development of accurate on-wafer, cryogenic characterization techniques", IEEE Transactions on Microwave Theory and Techniques, Vol. 44, No. 7, pp. 1178-1183, July 1996.

[9] C.R. Pollock, "Fundamentals of Optoelectronics", IRWIN Publishing, ISBN 0-256-10104-3.

[10] V. Hietala, K.L. Lear, M.G. Armendariz, C.P. Tigges, H.Q. Hou, and J.C. Zolper, "Electrical Characterization and Application of Very High Speed Vertical Surface Emitting Lasers (VCSELs)", IEEE MTT-S Digest, Vol. 1, pp. 355-358, 1997.